





RESEARCH ARTICLE

Guanabenz ameliorates disease in vanishing white matter mice in contrast to sephin1

Diede Witkamp^{1,2,a} , Ellen Oudejans^{1,2,a} , Gino V. Hu-A-Ng^{1,2}, Leoni Hoogterp^{1,2}, Aleksandra M. Krzywańska^{1,2}, Milo Žnidaršič^{1,2}, Kevin Marinus^{1,2} , Christina F. de Veij Mestdagh^{3,*}, Imke Bartelink⁴, Marianna Bugiani⁵, Marjo S. van der Knaap^{1,2,b} & Truus E. M. Abbink^{1,2,b} 

¹Child Neurology, Emma Children's Hospital, Amsterdam Leukodystrophy Center, Amsterdam University Medical Centers, Vrije Universiteit and Amsterdam Neuroscience, Amsterdam, The Netherlands

²Department of Integrative Neurophysiology, Center for Neurogenomics and Cognitive Research, VU University, Amsterdam, The Netherlands

³Department of Molecular and Cellular Neurobiology, Center for Neurogenomics and Cognitive Research, VU University, Amsterdam, The Netherlands

⁴Department of Pharmacy and Clinical Pharmacology, Amsterdam UMC, Location VUmc, Amsterdam, The Netherlands

⁵Department of Pathology, Amsterdam University Medical Centers, Vrije Universiteit and Amsterdam Neuroscience, Amsterdam, The Netherlands

Correspondence

Truus E. M. Abbink, Child Neurology, Emma Children's Hospital, Amsterdam Leukodystrophy Center, Amsterdam University Medical Centers, Vrije Universiteit and Amsterdam Neuroscience, Amsterdam, The Netherlands. Tel: +31 (0)20 5988292. E-mail: g.abbink@amsterdamumc.nl

Present address

*Alzheimer Center Amsterdam, VU University Medical Center, Amsterdam, The Netherlands

Funding Information

This study was supported by ELA grant 2017-02712 and ZonMW TOP grant 91211005.

Received: 23 March 2022; Revised: 2 June 2022; Accepted: 3 June 2022

Annals of Clinical and Translational Neurology 2022; 9(8): 1147–1162

doi: 10.1002/acn3.51611

^aEqual contribution.

^bShared senior author.

Abstract

Objective: Vanishing white matter (VWM) is a leukodystrophy, characterized by stress-sensitive neurological deterioration and premature death. It is currently without curative treatment. It is caused by bi-allelic pathogenic variants in the genes encoding eukaryotic initiation factor 2B (eIF2B). eIF2B is essential for the regulation of the integrated stress response (ISR), a physiological response to cellular stress. Preclinical studies on VWM mouse models revealed that deregulated ISR is key in the pathophysiology of VWM and an effective treatment target. Guanabenz, an α 2-adrenergic agonist, attenuates the ISR and has beneficial effects on VWM neuropathology. The current study aimed at elucidating guanabenz's disease-modifying potential and mechanism of action in VWM mice. Sephin1, an ISR-modulating guanabenz analog without α 2-adrenergic agonistic properties, was included to separate effects on the ISR from α 2-adrenergic effects. **Methods:** Wild-type and VWM mice were subjected to placebo, guanabenz or sephin1 treatments. Effects on clinical signs, neuropathology, and ISR deregulation were determined. Guanabenz's and sephin1's ISR-modifying effects were tested in cultured cells that expressed or lacked the α 2-adrenergic receptor. **Results:** Guanabenz improved clinical signs, neuropathological hallmarks, and ISR regulation in VWM mice, but sephin1 did not. Guanabenz's effects on the ISR in VWM mice were not replicated in cell cultures and the contribution of α 2-adrenergic effects on the deregulated ISR could therefore not be assessed. **Interpretation:** Guanabenz proved itself as a viable treatment option for VWM. The exact mechanism through which guanabenz exerts its ameliorating impact on VWM requires further studies. Sephin1 is not simply a guanabenz replacement without α 2-adrenergic effects.

Introduction

Vanishing white matter (VWM) is a leukodystrophy mainly presenting in young children.¹ It causes chronic neurological deterioration with episodes of major and rapid decline, provoked by different types of physical

stress. It leads to premature death and curative treatment is currently absent. Neuropathology includes white matter rarefaction, lack of adequate astrogliosis, deficient myelin, immature astrocytes, and oligodendrocytes in the white matter and mislocalized Bergmann glia.^{2,3} Dysfunction of astrocytes is central in the pathogenesis of VWM.⁴ VWM

is caused by bi-allelic pathogenic variants in the five genes (*EIF2B1–5*) encoding the subunits (α – ϵ) of the eukaryotic initiation factor 2B (eIF2B).⁵ eIF2B acts as the guanine nucleotide exchange factor for eIF2 and is as such conditional for the translation of mRNAs into proteins and for regulating protein synthesis rates.^{6,7} eIF2B orchestrates the integrated stress response (ISR), an adaptive response to different types of cellular stress.⁸ The ISR is activated by stimuli that cause phosphorylation of Ser51 in the α -subunit of eIF2. Phosphorylated eIF2 α inhibits eIF2B, thereby reducing protein synthesis rates, while at the same time upregulating expression of stress-resolving proteins.⁹ In VWM, eIF2B activity is reduced without significant impact on protein synthesis rates.^{10–15} In representative VWM mouse models, the ISR was found to be progressively deregulated in astrocytes.^{4,13,14,16} ISR deregulation is evident by increased expression of the transcription factor ATF4 in combination with reduced levels of phosphorylated eIF2 α , suggesting that cellular stress is absent or negligible. The increased ATF4 expression is accompanied by altered expression of ATF4-regulated genes.^{13,14,17} ISR deregulation has been confirmed in astrocytes in VWM patients' brains.¹³ ISR inhibition ameliorates VWM in mouse models,^{13,14} indicating that the deregulated ISR is central in VWM pathogenesis and is a viable drug target.

Guanabenz (GBZ), an FDA-approved antihypertensive drug, is an α 2-adrenergic receptor (α 2-AR) agonist; it acts on the ISR as a second target.^{18,19} A recent study showed that weekly injections with GBZ ameliorates Bergmann glia localization and myelin pathology in VWM mice.³ The study did not address the question how GBZ causes this improvement. Sephin1 (S1) is a GBZ derivative that lacks α 2-AR agonistic properties but shares the ISR-modulating property.²⁰ S1 has not been tested in VWM. Earlier studies using GBZ or S1 showed ISR-ameliorating effects in models of neurological diseases.^{20–25} For both compounds the mechanism of action is unclear. Both were initially thought to inhibit GADD34, causing increased eIF2 α phosphorylation and suppressed expression of ATF4 and its regulated genes.^{19,20,26} Recently, the GADD34 target has been challenged, but GBZ- and S1-induced ISR-ameliorating effects in models of neurological diseases have remained undisputed.²⁷ We hypothesized that GBZ and S1 would alleviate the clinical phenotype of VWM through an ameliorating effect on the deregulated ISR in astrocytes^{19,20} and that the parallel use of GBZ and S1 would help separate ISR effects from α 2-adrenergic effects. We tested both compounds in our VWM mouse model, and investigated clinical signs, neuropathological hallmarks as well as ISR deregulation. Additional tests were performed aimed at unraveling GBZ's mechanism of action in VWM.

Materials and Methods

Animals

Studies were performed with *2b5^{ho}* mice, which are homozygous for eIF2B ϵ Arg191His, and *2b4^{he}2b5^{ho}* mice, which are heterozygous for eIF2B δ Arg484Trp and homozygous for eIF2B ϵ Arg191His.^{4,13} Wild-type (WT) C57BL/6J mice were included as healthy controls. Mice were weaned at P21 and kept at a 12 h light/dark cycle with food and water provided ad libitum. Animal experiments were performed in compliance with the Dutch and European law and with approval of the local animal care and use committee of the VU University [licenses FGA 13–02, CCD AVD1120020172804, work-protocols 2804-NEU18-03A2, 2804-NEU19-12A5, 2804-NEU20-17]. Per breeding cycle, WT and VWM mice were evenly assigned to treatment groups based on their initial body weight to prevent a body weight bias.

Compound preparations

Guanabenz acetate (GBZ, Medichem) and sephin1 (S1, Axon Medchem) were dissolved in 100% PEG300 to 20 mg/ml and diluted with water-for-injection (WFI) to 0.45 mg/ml for S1 and GBZ (4.5 mg/kg injections), or 1 mg/ml for GBZ (10 mg/kg injections). The vehicle PEG300 was diluted to 2.25% in WFI and used as placebo.

Acute effects of GBZ and S1 on ISR markers

Male mice of indicated genotypes at indicated ages received a single intraperitoneal (i.p.) injection with placebo, 4.5 mg/kg GBZ, 10 mg/kg GBZ, or 4.5 mg/kg S1. Treatment groups comprised two or four animals per genotype per time point. Mice were terminated by cervical dislocation for tissue collection (Table S1).

Long-term treatment with GBZ or S1 and clinical assessments

Male WT and *2b4^{he}2b5^{ho}* mice received daily i.p. injections with placebo, 4.5 mg/kg GBZ, 4.5 mg/kg S1 or weekly with 10 mg/kg GBZ from an age of 7–8 weeks. Each treatment group consisted of 8 WT and 16 *2b4^{he}2b5^{ho}* mice. Body weight was monitored. Neurological deterioration was scored weekly before injection.²⁸ Motor skills were assessed on a 1.2-cm-wide balance beam after training on a 2.6-cm-wide beam,⁴ and on the CatWalk XT 10.6²⁹ after 10–11 weeks of injections. Mice did not receive treatment at these 2 days of motor skills testing to avoid α 2-adrenergic effects of GBZ. The day after the CatWalk test, animals received a final injection and were terminated by cervical

dislocation or PFA-perfusion approximately 4 h after injection, approximately two times the compound half-life of 1.8 h. Tissues were collected for postmortem analyses (Table S1). CatWalk data were included only if mice had a minimum of six consecutive steps without pauses or turns. Data were analyzed by researchers blinded to treatment and genotype.

Hypothermia quantification

Body temperature was measured to investigate α 2-adrenergic effects. Telemetric temperature probes (Anipill, Animals Monitoring, Hérouville, France) were implanted into the abdominal cavities of 2-month-old male WT and *2b4^{he}2b5^{ho}* mice.³⁰ Animals were injected subcutaneously with 0.05 mg/kg buprenorphine 30 min prior to surgery. Full anesthesia was applied during surgery (1.5%–3% isoflurane in oxygen). Post operation analgesia (buprenorphine 0.05 mg/kg) was provided. At least 7 days after surgery, mice received daily i.p. injections with placebo, 4.5 mg/kg GBZ, 4.5 mg/kg S1 or weekly with 10 mg/kg GBZ. Treatment groups consisted of 4 WT and 4 VWM mice. A hypothermia measure was determined based on temperature reduction and duration: After each injection, the area of the temperature curve under the baseline body temperature curve from placebo-injected genotype controls (AUC) was computed with GraphPad Prism 8.2.1.

Immunohistochemistry and immunofluorescence

Perfusion-fixed mouse brains were embedded in paraffin. Immunostainings to detect 4E-BP1, MOG, and S100 β were performed on 6- μ m-thick deparaffinized brain sections.^{4,29} The ratio of mislocalized:normally localized S100 β -positive Bergmann glia was determined.⁴ Immunofluorescence to detect nestin and GFAP was performed on fresh-frozen, 6- μ m-thick brain sections including corpus callosum⁴ with a 30-min blocking step. Nestin-GFAP double positive astrocytes and DAPI-positive nuclei in the corpus callosum were counted in four standardized fields per animal (2x rostrum and 2x splenium) and the percentage of nestin-GFAP double-positive cells over the total number of DAPI-positive nuclei was determined. Table S2 lists antibodies and staining details.

ISR quantification with qPCR and Western blot

Cerebella were prepared for qPCR and Western blot (Table S1).¹³ qPCR was performed^{15,29} with *Hprt* mRNA as reference. Oligonucleotide primers for *Hprt* mRNA

quantification are (5' \rightarrow 3'): GTTGGGCTTACCTCAC TGCT (forward) and TAATCACGACGCTGGGACTG (reverse). SDS-PAGE and Western blotting were performed^{15,31} with indicated primary antibodies (Table S2). HRP-labeled anti-IgG rabbit (1:10000, Dako, P0448) or HRP-labeled anti-IgG mouse (1:10000, Dako, P0447) were used as secondary antibody. Quantification was as described.¹⁵

Cell culture

Murine AtT-20 pituitary cell line (AtT-20/D16/16 CtT)³² was cultured with Dulbecco's modified Eagle medium (Gibco), 10% fetal bovine serum (HyClone/Thermoscientific) and 1% penicillin-streptomycin (Invitrogen). The recombinant AtT-20 cell line expressing the α 2-AR (subtype 2A)³³ was cultured in the same medium, although penicillin-streptomycin was replaced with geneticin as selective antibiotic (Gibco). Cells were kept in 5% CO₂/95% air at 37°C. To assess ISR effects, both cell lines were seeded in 25-cm² flasks and cultured until 80% confluency. Cells were treated with vehicle or 0.33 μ mol/L thapsigargin (Sigma) and co-treated with S1 and GBZ for 6 h. Cells were subsequently washed twice with ice-cold phosphate-buffered saline and collected in TRIzolTM (Invitrogen). RNA was isolated¹⁵ and qPCR was performed^{15,29} with *Akt* as reference. Oligonucleotide primers for *Adra2a* mRNA quantification are (5' \rightarrow 3'): AGATCAACGACCAGAAGTGGTA (forward) and AGACCAGGATCATGATGAGGCA (reverse).

Statistical analyses

The program Factor was used to correct for session variation within qPCR, Western blot, and cell culture experiments,³⁴ without correcting for variation in conditions (genotype, treatments). Statistical analyses were performed with GraphPad Prism 8.2.1 (Data S1). Differences were considered statistically significant when $p < 0.05$. VWM disease parameters were designated when statistically significant differences were observed between placebo-treated WT and VWM animals. If a significant difference was found, treatment effects were examined in WT and VWM animals separately with a one-way ANOVA, unpaired t -test or appropriate non-parametric alternative. Temperature data were assessed with paired t -tests, differences in GBZ dosage effects were assessed with a one-way ANOVA for WT and VWM animals separately with a one-way ANOVA, unpaired t -test or appropriate non-parametric alternative as indicated. CatWalk performance was analyzed using the software program R.³⁵ Data were analyzed using a two-way ANOVA followed by a Tukey's post hoc test for multiple comparisons. If these data did

not meet the assumptions for a two-way ANOVA and transformation with LOG10 also failed in meeting the assumptions, they were analyzed with a Kruskal–Wallis test followed by a Mann–Whitney's post hoc test. Individual CatWalk parameters were categorized as described.³⁵

Results

Single dose of GBZ has a temporary impact on ISR deregulation in VWM mouse brain

Previously, weekly injections with 10 mg/kg GBZ ameliorated brain pathology in VWM mice.³ To assess brain ISR effects, WT and $2b5^{ho}$ mice received a single injection of saline or 10 mg/kg GBZ and were terminated 4 or 24 h later. In VWM mouse brains, eIF2 α phosphorylation levels are lower than in control mice, previously explained by an increased production of GADD34 as a consequence of reduced eIF2B activity.^{13,36,37} Considering the presumed GADD34 inhibitory effect of GBZ, it was against our expectations that GBZ reduced brain eIF2 α phosphorylation in WT (-31% , $p = 0.1328$) and $2b5^{ho}$ (-33% , $p = 0.0763$) mouse brain at 4 h post injection with recovery to baseline at 24 h post injection (Fig. 1), suggesting that a temporary stimulation of eIF2B occurs as downstream effect. In line with this, the levels of ATF4-regulated mRNAs *Ddit3* and *Trib3* in $2b5^{ho}$ mice were reduced by GBZ as compared to placebo, reaching significant reduction at 24 h post injection (*Ddit3*: -27% , $p = 0.0293$, *Trib3*: -34% , $p = 0.0051$). Such a reduction was not observed in WT mice, probably because they lack the constitutive ATF4 activation present in $2b5^{ho}$ mouse brain.¹³ Surprisingly and in contrast to the otherwise reduced ATF4-regulated mRNAs, the expression of the ATF4-regulated *Gadd34* mRNA was temporarily increased in WT and $2b5^{ho}$ mice 4 h post injection (WT: $+40\%$, $p = 0.01$, $2b5^{ho}$: $+28\%$, $p = 0.0339$).

Considering GBZ's half-life in plasma in mice is 1.8 h³⁸ and the effects on some ISR markers attenuate after 24 h (Fig. 1), weekly 10 mg/kg GBZ-regimen is a suboptimal dosing schedule for establishing therapeutic effects in mice. Based on this information we selected a daily dose

of 4.5 mg/kg.³⁸ A single injection of 4.5 mg/kg or 10 mg/kg GBZ in $2b4^{he}2b5^{ho}$ mice temporarily reduced eIF2 α phosphorylation in a dose-dependent manner: -33% for 4.5 mg/kg ($p = 0.0725$) and -50% for 10 mg/kg ($p = 0.0391$; Fig. 2). A single injection with 4.5 mg/kg S1 temporarily reduced eIF2 α phosphorylation (-40% , $p = 0.0569$).

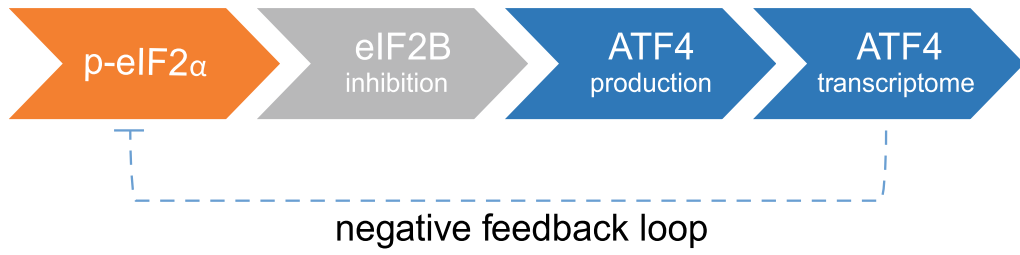
GBZ induces hypothermia with rapid, but incomplete habituation on daily injections

A single GBZ injection transiently sedated WT and $2b4^{he}2b5^{ho}$ mice, as expected for an $\alpha 2$ -AR agonist.³⁹ S1 did not sedate VWM mice. To assess $\alpha 2$ -adrenergic effects on body temperature, the temperature of WT and $2b4^{he}2b5^{ho}$ mice was monitored when injected daily with placebo vehicle, 4.5 mg/kg GBZ or S1, or weekly with 10 mg/kg GBZ (Fig. S1). Baseline body temperatures of WT and $2b4^{he}2b5^{ho}$ mice differed subtly, but they changed similarly for each treatment (Fig. 3). Placebo and S1 injections did not affect body temperature in either genotype.⁴⁰ The first GBZ injection caused transient hypothermia in both genotypes at both dosages. With consecutive daily GBZ injections hypothermia in WT and $2b4^{he}2b5^{ho}$ mice diminished and stabilized as compared to the first injection: Hypothermia after the third and following injections was reduced by more than 50% compared to the first injection (Fig. S1 and Data S1). The minimum body temperature did not differ after each GBZ injection, indicating that AUC reduction was due to shortened duration of the hypothermia. Our observations indicate rapid, although not entirely complete habituation to GBZ's $\alpha 2$ -adrenergic effects with the 4.5 mg/kg daily regimen, but not with the weekly with 10 mg/kg GBZ regimen.

GBZ ameliorates clinical signs in VWM mice and S1 does not

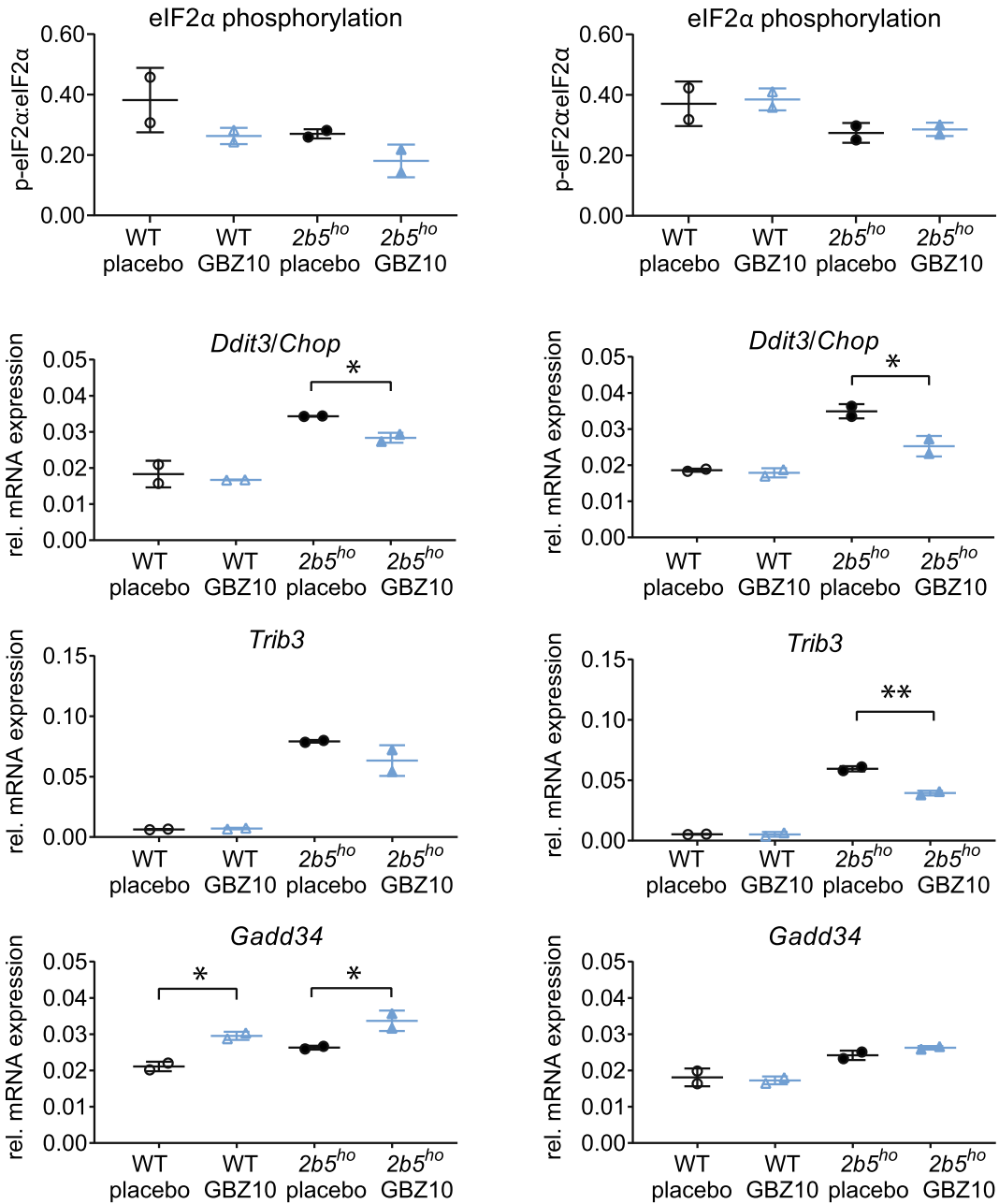
To assess GBZ and S1 effects on disease hallmarks, WT, and $2b4^{he}2b5^{ho}$ mice were injected daily with placebo, 4.5 mg/kg GBZ, 4.5 mg/kg S1 or weekly with 10 mg/kg

Figure 1. One i.p. injection with 10 mg/kg GBZ reduces ATF4 transcriptome in WT and $2b5^{ho}$ mice. Four-month-old male WT (open symbols) and early symptomatic $2b5^{ho}$ mice (closed symbols) received one i.p. injection of saline (placebo, black) or 10 mg/kg GBZ (blue). Mice were terminated 4 or 24 h after injection. Brains were taken out and sagittally cut. One half was lysed to obtain protein samples and total RNA samples as described.^{15,29} Western blot and qPCR were performed for indicated ISR markers (*Akt* was used as reference in qPCR).¹³ A simplified overview of the ISR pathway is shown; *Ddit3/Chop*, *Trib3*, and *Gadd34* are part of the ATF4-regulated transcriptome. GADD34 is part of the negative feedback loop and dephosphorylates eIF2 when bound to protein phosphatase 1c. Graphs show individual and mean values, \pm SD. qPCR and Western blot samples were derived from the same mouse. $n = 2$ animals per treatment group. Statistically significant differences between placebo-treated WT and placebo-treated $2b5^{ho}$ mice are not indicated. Treatment effects on protein levels were statistically analyzed with an unpaired *t*-test. * $p < 0.05$, ** $p < 0.01$.



4 hours post injection

24 hours post injection



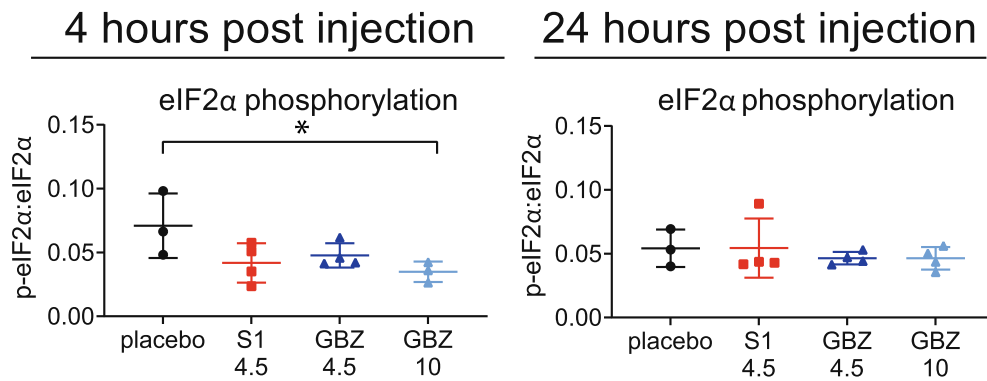


Figure 2. One i.p. injection with 4.5 mg/kg S1, 4.5 or 10 mg/kg GBZ transiently reduces eIF2 α phosphorylation in $2b4^{he}2b5^{ho}$ mice. Two-and-a-half-month-old male early symptomatic $2b4^{he}2b5^{ho}$ mice received one i.p. injection of 2.25% PEG300, 4.5 or 10 mg/kg GBZ. Mice were terminated 4 or 24 h after injection. Brains were taken out. Cerebella were lysed and samples were subjected to SDS-PAGE and Western blot to detect Ser51-phosphorylated eIF2 α and total eIF2 α . Graphs show individual and mean values, \pm SD. Results were statistically analyzed with an unpaired *t*-test. **p* < 0.05.

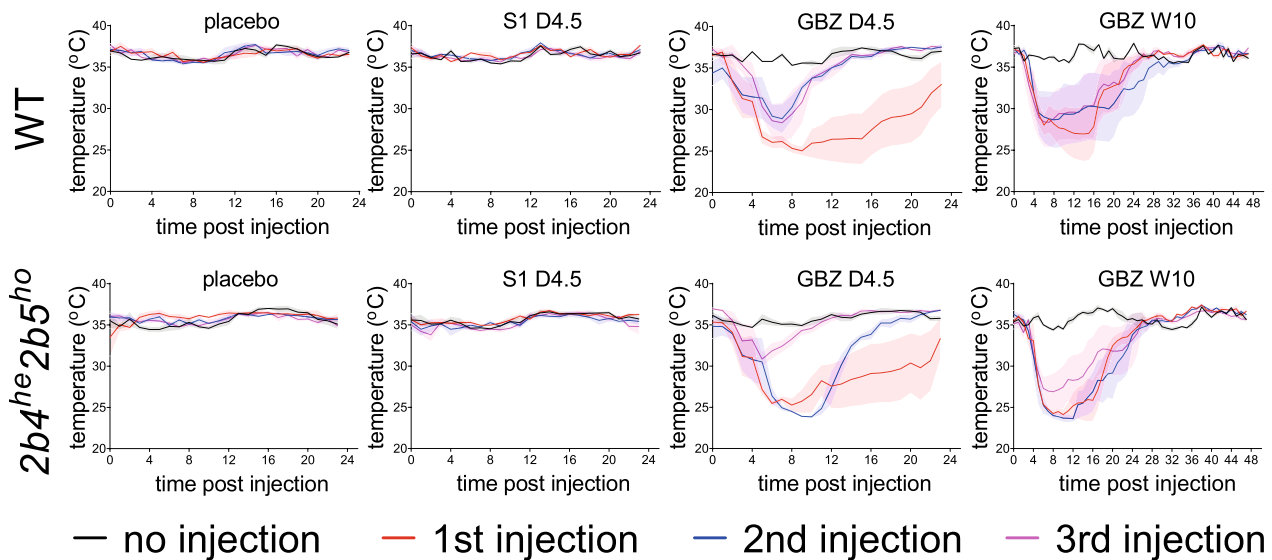


Figure 3. GBZ injection causes temporary hypothermia similarly in WT as in $2b4^{he}2b5^{ho}$ mice. Temperature loggers were inserted in 2-month-old, male WT and pre-symptomatic $2b4^{he}2b5^{ho}$ mice. Treatments of daily injection with 2.25% PEG300 (placebo), 4.5 mg/kg S1 (S1 D4.5), 4.5 mg/kg GBZ (GBZ D4.5) or weekly injection with 10 mg/kg GBZ (GBZ W10) were started 1 week after surgery. Injections were placed alternating on left- or right-hand side of the abdominal midline. Body temperature was registered once per hour (h). Temperature at time point 0 was recorded directly before each injection. Graphs show mean body temperature \pm SEM. Body temperature is shown for the first three consecutive injections, which follow a daily or weekly interval. Injection of 10 mg/kg GBZ lowered body temperature for more than 24 h, which is the reason for showing a 48-h time window. Mean baseline temperature for WT and $2b4^{he}2b5^{ho}$ mice were determined from placebo-injected animals (WT, 36.6°C, $2b4^{he}2b5^{ho}$, 35.4°C) and used for AUC calculations for each injection per animal. AUCs are shown in Figure S1.

GBZ for 10–12 weeks. At the start, mice were approximately 7 weeks old, at which time the ISR is deregulated, white matter damage is subtle and clinical neurological features have not yet appeared in $2b4^{he}2b5^{ho}$ mice.^{3,4,13}

Body weight is reduced in $2b4^{he}2b5^{ho}$ mice and was monitored during treatment. Daily GBZ injections reduced body weight gain in WT mice by 77% compared to daily placebo (*p* = 0.0001; Fig. 4A; Data S1), but

increased body weight gain in $2b4^{he}2b5^{ho}$ mice by 13% (*p* = 0.1125). Body weight of $2b4^{he}2b5^{ho}$ mice was not affected by daily S1 or weekly GBZ treatments.

Mean neurological decline as expressed in the neuroscore was reduced to 49% in daily and to 29% weekly GBZ-treated $2b4^{he}2b5^{ho}$ mice (*p* = 0.0085 and *p* = 0.2251, respectively; Fig. 4B; Data S1). Most strikingly, both GBZ regimens effectively ameliorated ataxia (Fig. 4C and D;

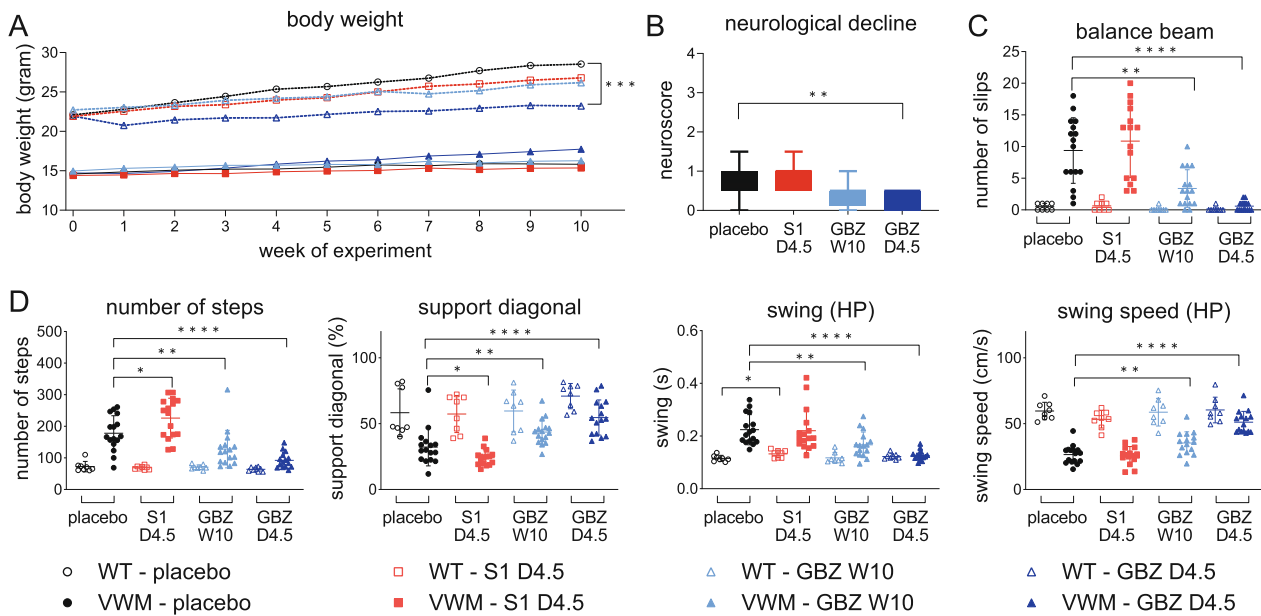


Figure 4. GBZ ameliorates clinical signs in $2b4^{he}2b5^{ho}$ mice. Eight WT (open symbols) and 16 $2b4^{he}2b5^{ho}$ (VWM) mice (closed symbols) were injected daily with placebo (2.25% PEG300), 4.5 mg/kg S1 (S1 D4.5), 4.5 mg/kg GBZ (GBZ D4.5) or weekly with 10 mg/kg GBZ (GBZ W10) from an age of 6–8 weeks onwards. Injections were placed alternating on left- or right-hand side of the abdominal midline. One mouse displayed signs of epilepsy 2 days after daily injections with 4.5 mg/kg GBZ, was found dead the day after and was omitted from the study. Autopsy did not show signs of infection or other causes for early demise. Graphs show mean phenotypic measures: (A) body weight; (B) neuroscores in VWM mice indicating neurological deterioration; (C) number of slips on balance beam (one S1-treated VWM mouse was unable to traverse the balance beam and was excluded from analysis); D–G, gait parameters on the CatWalk in different categories (HP, hind paws): (D) run characterization; E, inter-limb coordination; F, temporal; G, kinetic. Neuroscores are 0 in all WT mice (not plotted). Treatment effects by GBZ and S1 were analyzed only for parameters that statistically differed between placebo-treated WT and placebo-treated VWM mice. Statistical analyses investigating compound-related differences in body weight were performed with a repeated measures two-way ANOVA followed by post hoc Dunnett's correction. Balance beam performance was examined with a Welch's ANOVA and a Dunnett's correction and neuroscore with a Kruskal–Wallis test followed by Dunn's correction. CatWalk data was analyzed with a Kruskal–Wallis with Mann–Whitney U correction. * $p < 0.05$, ** $p < 0.01$, *** $p < 0.001$, **** $p < 0.0001$.

Data S1–S4). Daily GBZ injections in $2b4^{he}2b5^{ho}$ mice normalized balance beam performance and several gait parameters in CatWalk tests. Placebo- and S1-treated $2b4^{he}2b5^{ho}$ mice showed similar neurological decline and number of slips on the balance beam, perhaps subtly increased for S1 (+16%, $p = 0.8330$). Remarkably, 12 out of 16 S1-treated $2b4^{he}2b5^{ho}$ mice showed signs of tremor earlier than placebo-treated genotype controls, suggestive of subtle worsening. The latter is in line with mild worsening of some gait parameters in S1-treated $2b4^{he}2b5^{ho}$ mice (Fig. 4D). Neuroscores, balance beam performance, and gait parameters in WT mice were not affected by GBZ or S1, except for the increased hind paw swing in S1-treated WT mice (Fig. 4B–D, Data S1 and S5–S7).

Daily GBZ ameliorates neuropathological hallmarks of VWM and S1 does not

VWM neuropathological hallmarks^{3,4,13} were evident in placebo-treated $2b4^{he}2b5^{ho}$ mice (Figs. 5 and 6). These

were improved by daily GBZ injections, but not by daily S1 or weekly GBZ injections. Daily GBZ treatment reduced the mean percentage of mislocalized Bergmann glia in $2b4^{he}2b5^{ho}$ mice by 23% ($p = 0.0179$, Fig. 5) and the number of nestin-GFAP double positive immature astrocytes in the corpus callosum by 42% ($p = 0.0589$, Fig. 6A). Interestingly, the latter reduction was 54% in the splenium ($p = 0.029$) and 10% in the rostrum ($p = 0.185$). Small reductions were observed in the splenium after daily S1 and weekly GBZ treatment compared to placebo treatment (–11% and –38%, respectively) without statistical significance ($p = 0.896$ and 0.154 , respectively). Regarding treatment effects on myelin pathology, the mature oligodendrocyte markers *Mbp* and *Mog* mRNA and MBP and MOG protein levels were similar in cerebella from placebo-treated and GBZ- or S1-treated $2b4^{he}2b5^{ho}$ mice (data not shown), but immunohistochemistry for MOG protein showed that daily GBZ treatment improved myelin appearance in $2b4^{he}2b5^{ho}$ corpus callosum (Fig. 7), more so in splenium than in

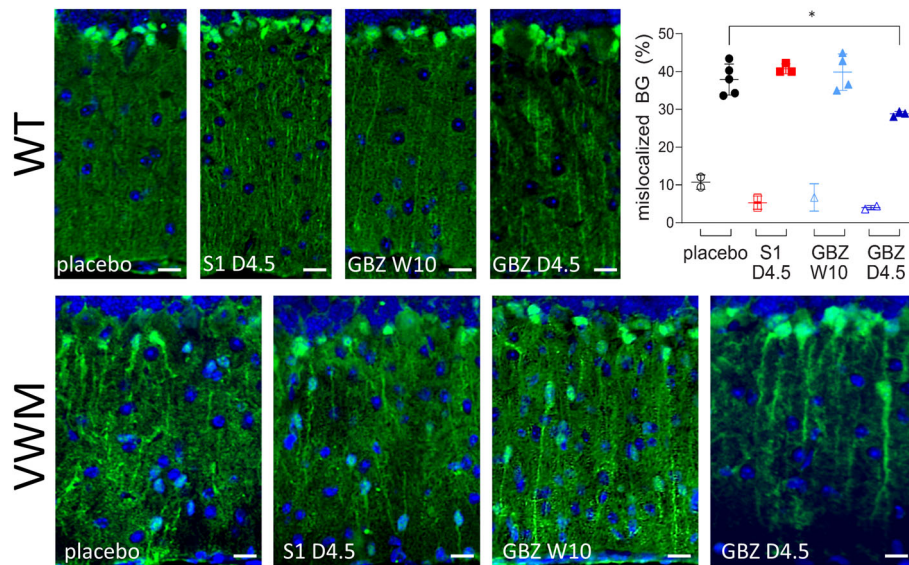


Figure 5. Daily GBZ 4.5 mg/kg reduces Bergmann glia mislocalization in $2b4^{he}2b5^{ho}$ mice. WT (open symbols) and $2b4^{he}2b5^{ho}$ (VWM) mice (closed symbols) were injected daily with placebo, 4.5 mg/kg S1 (S1 D4.5), 4.5 mg/kg GBZ (GBZ D4.5) or weekly with 10 mg/kg GBZ (GBZ W10). Sagittally cut brain sections were subjected to immunostaining for S100 β (green) and nuclear staining with DAPI (blue). Bergmann glia are double positive for S100 β and nuclear DAPI staining. Numbers of mice are $n = 2$ for WT placebo, WT S1 D4.5, and WT GBZ D4.5, $n = 1$ for WT GBZ W10, $n = 5$ for VWM placebo, $n = 3$ for VWM S1 D4.5 and VWM GBZ D4.5 and $n = 4$ for VWM GBZ W10. Per mouse 3–6 images were taken. Images show illustrative examples of Bergmann glia localized in the Purkinje layer in WT mice and in the Purkinje and molecular layers in $2b4^{he}2b5^{ho}$ mice. Bergmann glia were counted in the Purkinje layer (normal location) and in the molecular layer (mislocalized) by a blinded researcher. Percentages of mislocalized Bergmann glia were determined by dividing the number of mislocalized by the total number of Bergmann glia (100%). Graph shows individual and mean percentages of mislocalized Bergmann glia \pm SD. The percentage of mislocalized Bergmann glia in placebo-treated $2b4^{he}2b5^{ho}$ mice is significantly higher than in WT controls ($p < 0.001$; nested t -test; not indicated). Treatment effects on Bergmann glia mislocalization were assessed with a nested one-way ANOVA followed by Dunnett's correction. * $p < 0.05$. White bars, 15 μ m.

rostrum, in line with GBZ's differential effects on immature astrocyte numbers in these regions (Fig. 6B). In general, histological effects were not observed in WT brain for any of the tested compounds (Figs. 5 and 6; Fig. S2).

GBZ and S1 reduce eIF2 α phosphorylation in VWM mouse cerebella but only GBZ reduces expression of the ATF4 transcriptome

In VWM mouse brains, eIF2 α phosphorylation levels are lower than in control mice.¹³ GBZ and S1 reduced these levels further in $2b4^{he}2b5^{ho}$ cerebella as compared to placebo (mean change for GBZ weekly: -47% , $p = 0.0646$; GBZ daily: -51% , $p = 0.0361$; and S1 daily: -48% , $p = 0.0201$; Fig. 8). eIF2 α phosphorylation in WT mice was only decreased by GBZ (one-way ANOVA $F(3, 5) = 6306$, $p = 0.0375$) and not by S1, although post hoc testing yielded no significant results for GBZ either (mean change for GBZ weekly: -35% , $p = 0.0847$; GBZ daily: -28% , $p = 0.1581$; and S1 daily: $+7\%$, $p = 0.8681$; Fig. 8). Both daily and weekly GBZ regimens reduced expression of ATF4-regulated mRNAs in $2b4^{he}2b5^{ho}$ cerebella (e.g. mean reduction by 22% and 28% for *Ddit3*

and *Trib3* expression in daily injected mice), strikingly except for *Gadd34* mRNA expression, which was unchanged. By contrast, S1 did not affect expression of ATF4-regulated mRNAs in $2b4^{he}2b5^{ho}$ cerebella. The expression of ATF4-regulated mRNAs in WT mice was not changed by S1 or GBZ, although *Gadd34* mRNA level was subtly increased by daily GBZ compared to the placebo ($+33\%$, $p = 0.0554$ for daily 4.5 mg/kg; $+23\%$, $p = 0.1618$ for weekly 10 mg/kg; Data S1).

To verify if the differential GBZ effects on histopathology within the corpus callosum in VWM mice (Figs. 6 and 7) were associated with differential ISR deregulation, immunohistochemistry for the ISR marker 4E-BP1^{13,41} was performed in placebo- and daily GBZ-treated VWM mice. GBZ reduced the expression of this ISR marker more in the splenium than in the rostrum (Fig. S3).

Addressing GBZ's mechanism of action

S1 is an analog of GBZ, presumably with a shared target in the ISR. Effects of S1 and GBZ in $2b4^{he}2b5^{ho}$ mice were therefore expected to be the same, but GBZ injections ameliorated clinical signs in $2b4^{he}2b5^{ho}$ mice and S1

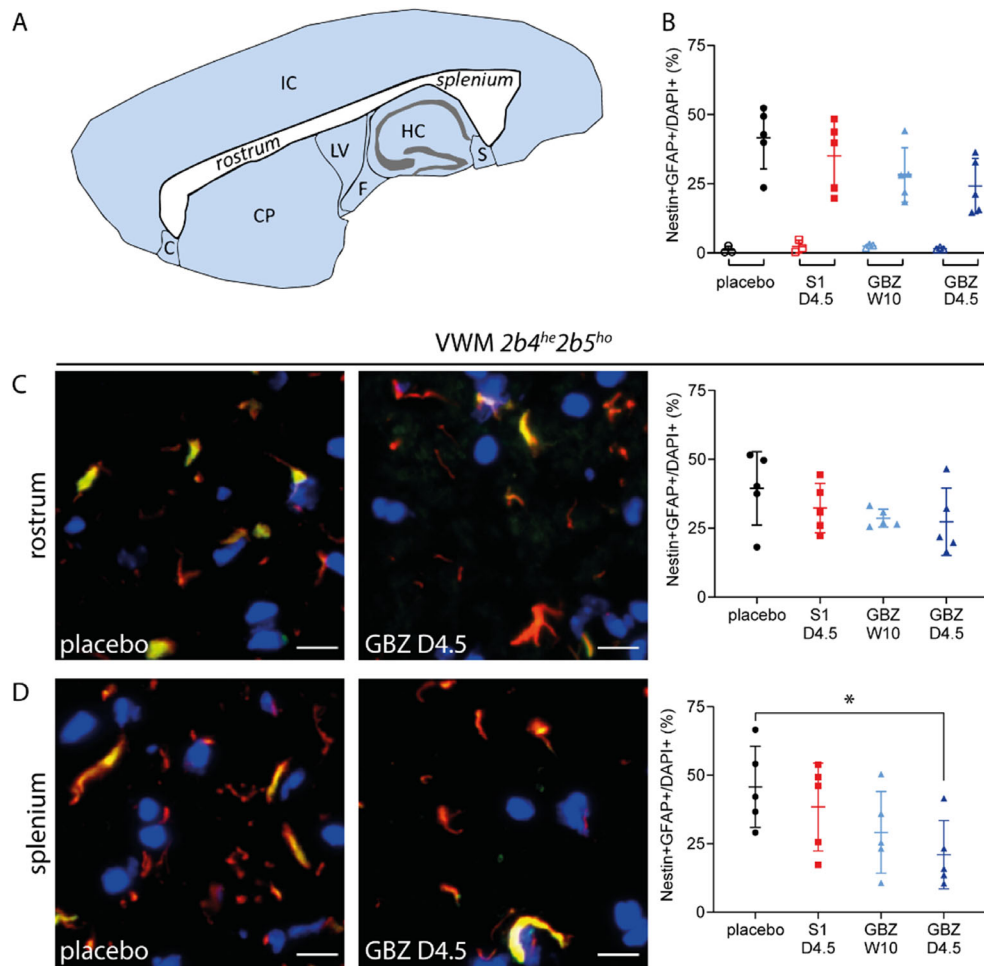


Figure 6. Daily GBZ 4.5 mg/kg regionally reduces number of immature astrocytes in the corpus callosum in $2b4^{he}2b5^{ho}$ mice. WT and $2b4^{he}2b5^{ho}$ mice were injected daily with placebo, 4.5 mg/kg S1 (S1 D4.5), 4.5 mg/kg GBZ (GBZ D4.5) or weekly with 10 mg/kg GBZ (GBZ W10). Sagittally cut brain sections of 3 WT (open symbols) and 5 VWM (closed symbols) mice were stained for nestin (green), GFAP (red), and nuclei (DAPI, blue). Counts of nestin-GFAP double positive astrocytes (orange) and DAPI-positive nuclei were determined in two images per rostrum and per splenium of the corpus callosum of each section. (A) Sagittal view of the corpus callosum (shown in white) with the rostrum located anterior and the splenium posterior. (B) Graph shows individual and mean percentages of nestin-GFAP double positive astrocytes in the corpus callosum \pm SD per genotype and treatment. (C and D) Images show representative stainings of VWM brains in indicated sections per indicated treatments. Graphs show percentages of nestin-GFAP double positive astrocytes in the rostrum (upper panel) or splenium (lower panel) in VWM mice \pm SD. Treatment effects on nestin-GFAP double positive astrocytes were assessed with one-way ANOVA. Treatment effects on nestin-GFAP double positive astrocytes in the splenium were corrected with post hoc Dunnett's. C, claustrum; CP, caudoputamen; F, fornix; HC, hippocampus; IC, iso-cortex; LV, lateral ventricle; S, subiculum * $p < 0.05$. White bars, 20 μ m.

injections did not. GBZ and S1 have similar pharmacological properties, with short half lives in plasma, similar accumulation in rodent brain, and similar ISR-modulating potencies in vitro.^{19,20,38} Both compounds reduced eIF2 α phosphorylation, but the expected associated reduced expression of the ATF4-regulated transcripts in $2b5^{ho}$ and $2b4^{he}2b5^{ho}$ mice was only seen for GBZ and not for S1. It is currently unclear how S1 reduced phosphorylated eIF2 α levels without reducing ATF4.

Our observations placed GBZ's main target, the $\alpha 2$ -AR, as a potential driver of eIF2B-ameliorating effects in VWM mice. If so, GBZ would alter ATF4-regulated mRNA levels differentially in the absence or presence of the $\alpha 2$ -AR. We tested this hypothesis with the mouse pituitary cell line AtT-20 that does not express $\alpha 2$ -AR and a recombinant derivative that expresses $\alpha 2$ -AR³³ (Fig. S4A). Both cell lines were subjected to GBZ or S1 in the absence or presence of the chemical thapsigargin that

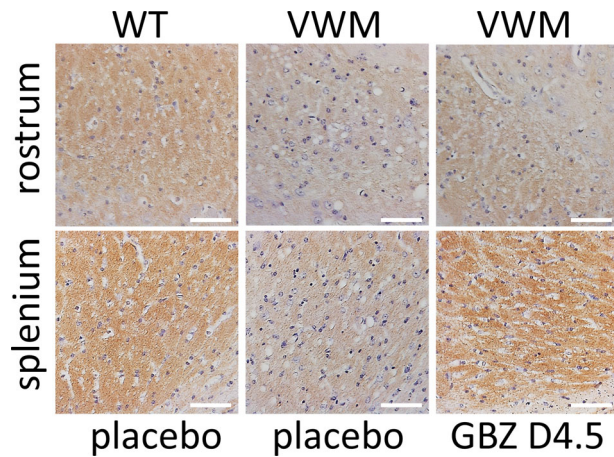


Figure 7. Daily GBZ 4.5 mg/kg regionally ameliorates myelin pathology the corpus callosum in $2b4^{he}2b5^{ho}$ mice. WT and $2b4^{he}2b5^{ho}$ (VWM) mice were injected daily with placebo, 4.5 mg/kg S1 (S1 D4.5), 4.5 mg/kg GBZ (GBZ D4.5) or weekly with 10 mg/kg GBZ (GBZ W10). Sagittally cut brain sections of 2 WT and 2 VWM mice were stained for MOG (brown) and counter stained with H&E (purple, indicating nuclei). Images show representative stainings of indicated sections per indicated treatment. Images are from the same section and represent one mouse per condition. White bars, 50 μ m.

causes ER stress, ISR activation, and splicing of the *Xbp1* mRNA. GBZ and S1 did not alter the expression of ATF4-regulated mRNAs in the absence of thapsigargin and similarly decreased their expression in the presence of thapsigargin (Fig. 9). GBZ and S1 similarly reduced *Xbp1* mRNA splicing in thapsigargin-treated AtT-20 (Fig. S4B).⁴² The absence or presence of the $\alpha 2$ -AR did not significantly impact on the inhibition of the expression of ATF4-regulated mRNAs nor the degree of *Xbp1* splicing inhibition. A particular role of the $\alpha 2$ -AR in GBZ's ISR-regulating and disease-ameliorating effects in VWM mice remained unidentified in these cell-based experiments.

Discussion

GBZ previously showed to improve brain pathology in VWM mice.³ The current study shows its ameliorating effects on clinical signs in VWM mice. Neurological decline and ataxia in $2b4^{he}2b5^{ho}$ mice are greatly improved with GBZ injections, more so with daily 4.5 mg/kg than weekly 10 mg/kg. Untreated VWM mice show a reduced body weight gain, which improves on successful treatment. GBZ increases body weight gain in VWM mice, but less so than seen with previous successful ISR-modulating treatments.^{13,14} Daily GBZ-treated WT animals show a reduction in body weight gain probably due to GBZ's sedative or hypothermic effects.^{43–45} These

effects have probably curbed a GBZ-induced body weight gain in VWM mice, obscuring its full beneficial potential on weight gain. The study shows GBZ's beneficial effect on VWM brain pathology hallmarks for the daily dosing schedule. How GBZ leads to differential effects in splenium versus rostrum remains to be deciphered; considering the striking clinical improvements, the difference does not seem clinically relevant. The experiments confirm a beneficial effect of GBZ therapy on ATF4 activation in the brain of VWM mice. Untreated VWM mice show activation of the ISR downstream of eIF2B with increased expression levels of ATF4-regulated mRNAs, including *Chop*, *Trib3*, and *Gadd34*, but decreased eIF2 α phosphorylation, previously explained by activation of GADD34 and absence of ISR activation by stress.¹³ In this study, however, GBZ-treated VWM mice show diminished overexpression of *Chop* and *Trib3*, but strikingly not of *Gadd34*. The latter probably causes further reduction of eIF2 α phosphorylation. In addition to effects on the ISR, GBZ has clear $\alpha 2$ -adrenergic effects with initial sedation and reduced body temperature; both show rapid habituation on daily dosing, although some effect on body temperature remains.

Presumably, S1 shares the effect on the ISR with GBZ, while lacking the $\alpha 2$ -adrenergic effect and was included in the study to isolate the two effects. As expected, S1 lacks all $\alpha 2$ -adrenergic effects and has no impact on alertness and body temperature in VWM mice. Against expectations, however, S1 does not have any beneficial effect on motor performance and body weight gain in VWM mice; if anything it may even worsen some clinical parameters. In line with these findings, S1 does not improve brain pathology in VWM mice. Regarding its impact on the ISR, it decreases eIF2 α phosphorylation, similar to GBZ, but levels of ATF4-regulated mRNAs including *Chop*, *Trib3*, and *Gadd34*, are unchanged, in contrast to GBZ.

Initially, GBZ and S1 were described to modulate the ISR caused by ER stress via GADD34 inhibition causing increased phosphorylated eIF2 α levels.^{19–21} Later studies contradicted the inhibitory effect of either drug on GADD34.^{22,27,42,46} Our study shows that both GBZ and S1 decrease phosphorylated eIF2 α in VWM brain, while GBZ increases *Gadd34* expression in WT and $2b5^{ho}$ mice and S1 does not. Those findings increase doubt on their GADD34-inhibiting effects as shared mechanism to decrease phosphorylated eIF2 α . Dephosphorylation of eIF2 α is executed by phosphatase 1c bound to a substrate-specifying co-factor, either CReP or GADD34.^{47–51} CReP operates under basal conditions and its expression is not regulated by eIF2B or ATF4, in contrast to GADD34.^{37,51} *Crep* expression was unaltered in $2b5^{ho}$ and $2b4^{he}2b5^{ho}$ brain and white matter tissue from VWM patients.¹³ GBZ nor S1 increased *Crep* expression

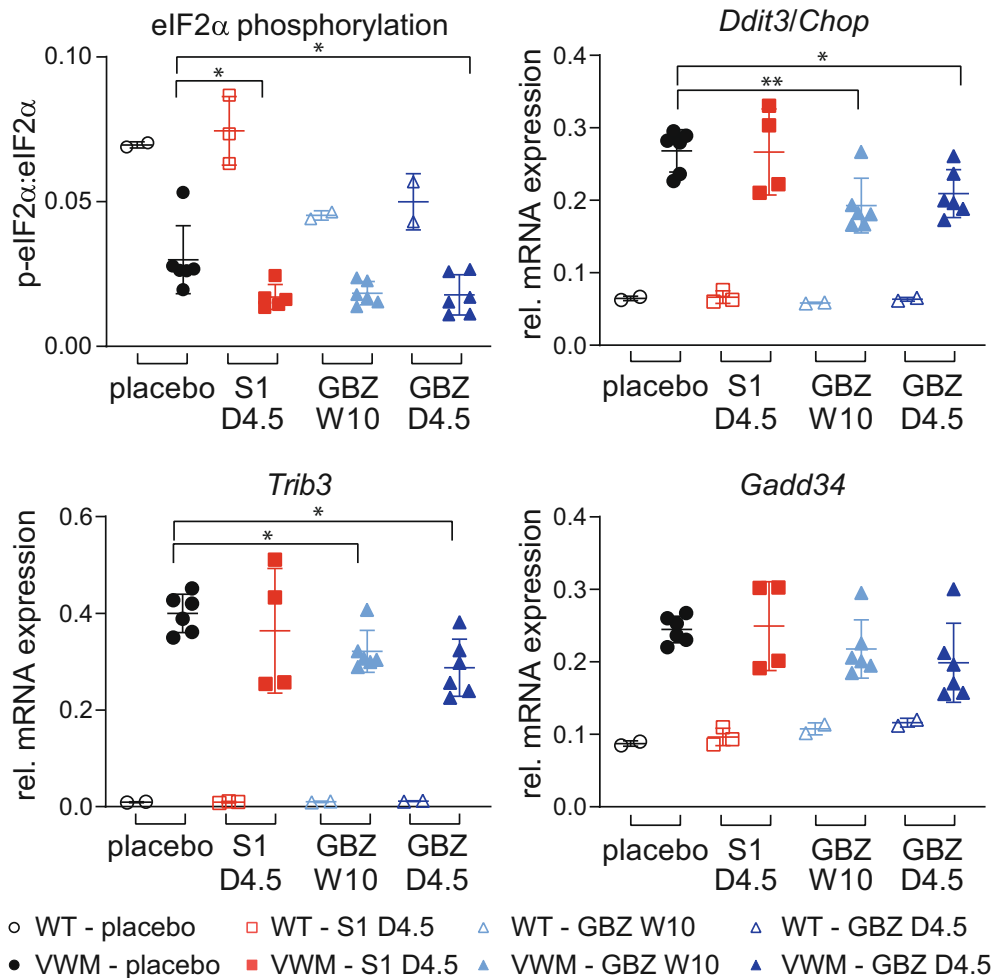


Figure 8. GBZ attenuates ISR parameters in $2b4^{he}2b5^{ho}$ mouse cerebella. WT (open symbols) and $2b4^{he}2b5^{ho}$ (VWM, closed symbols) mice were injected daily with placebo, 4.5 mg/kg S1 (S1 D4.5), 4.5 mg/kg GBZ (GBZ D4.5) or weekly with 10 mg/kg GBZ (GBZ W10) from an age of 6–8 weeks onwards for at least 10 weeks. ISR mRNA expression and eIF2 α phosphorylation were quantified with qPCR (*Hprt* as reference) and Western blot in $n = 2–3$ WT and $n = 4–6$ $2b4^{he}2b5^{ho}$ VWM cerebella, respectively. RNA and proteins samples were derived from the same cerebellar lysate. Graphs indicate individual data points and means \pm SD. Shown ISR markers differ significantly in placebo-treated WT versus placebo-treated VWM mice ($p < 0.05$; not indicated). Treatments effects on ISR markers were statistically analyzed with a one-way ANOVA followed by post hoc Dunnett's correction. eIF2 α phosphorylation findings in WT were statistically analyzed with a one-way ANOVA followed by post hoc Dunnett's correction ($p = 0.0375$) and in VWM mice with a Kruskal–Wallis test followed by post hoc Dunn's correction ($p = 0.0207$). * $p < 0.05$, ** $p < 0.01$.

in WT or VWM mice,¹³ ruling a CREP-related mechanism out as explanation for the decrease in eIF2 α phosphorylation. Of note, the striking ameliorating clinical effect of GBZ on VWM mice and lack of clinical effect of S1 indicate that diminished eIF2 α phosphorylation by itself does not ameliorate VWM. This conclusion is in line with other preclinical studies, which report ameliorating effects of S1 in a multiple sclerosis mouse model and of ISRIB and 2BAct in VWM mouse models without noticeable changes in eIF2 α phosphorylation.^{13,14,22} The observation that GBZ effects on eIF2 α phosphorylation

are similar in WT and VWM mice, while S1 effects are seen in VWM mice, but not in WT mice, suggests that GBZ's target is present in both genotypes, while S1's target is not sufficiently expressed or has opposite effects in WT brain, questioning that GBZ and S1 have the same targets. Alternatively, the temporary ATF4 attenuation by GBZ and S1 occurs through a shared target but progresses at different rates. Reduced eIF2 α phosphorylation is expected to release eIF2B activity and attenuate the expression of ATF4-regulated mRNAs, which we indeed observed in GBZ-treated but not in S1-treated $2b4^{he}2b5^{ho}$

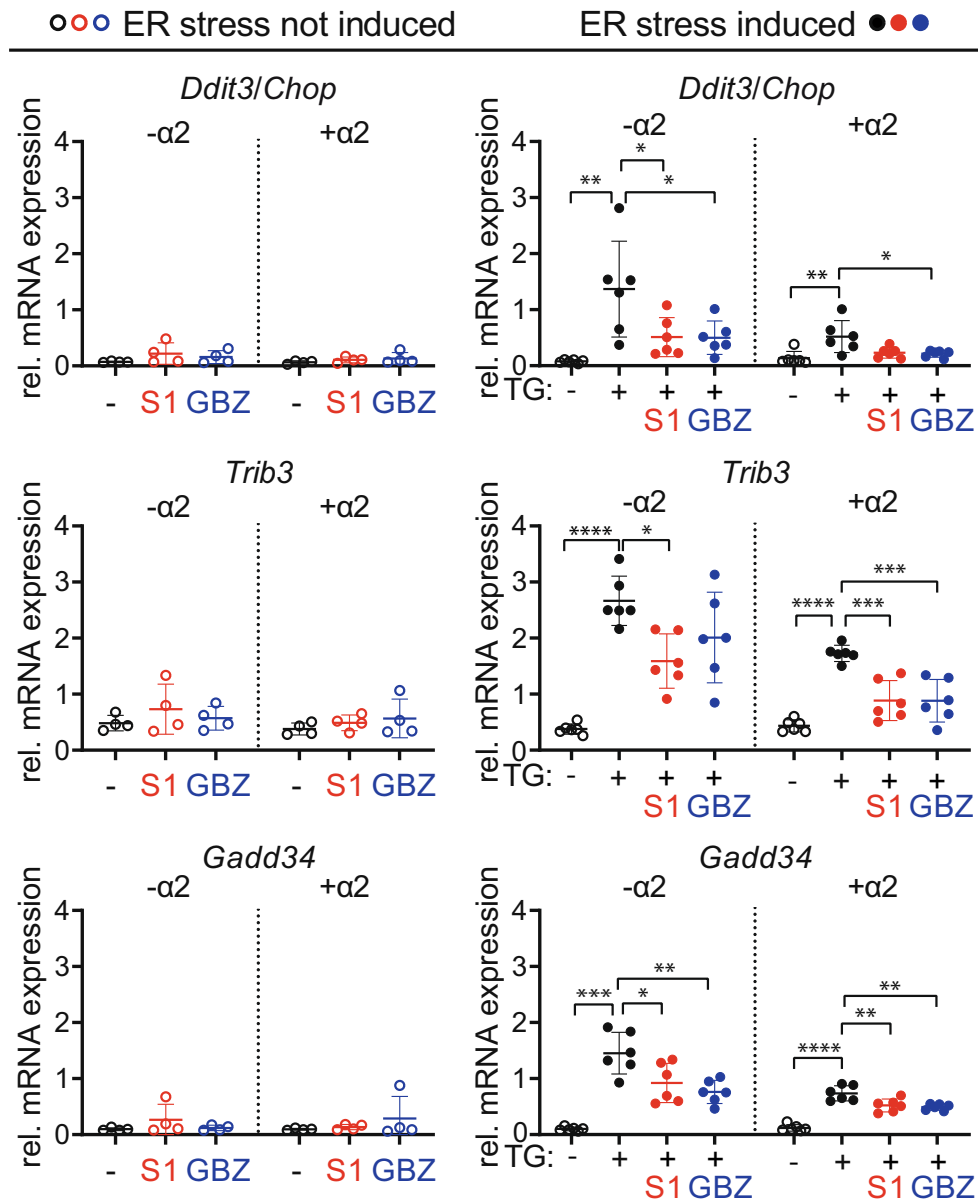


Figure 9. GBZ and S1 attenuates ISR parameters similarly in the absence or presence of the $\alpha 2$ -AR. AT-20 cells that express ($+\alpha 2$) or not express ($-\alpha 2$) the $\alpha 2$ -AR subtype 2A were treated with vehicle (-) or thapsigargin (TG: +) for 6 h, in the presence or absence of 50 $\mu\text{mol/L}$ S1 or GBZ to induce ER stress. ISR mRNA marker expression was quantified with qPCR (*Akt* as reference). Graphs indicate individual data points and means \pm SD. Shown ISR markers differ significantly in vehicle-treated versus TG-treated cells, as analyzed with an unpaired *t*-test or the appropriate non-parametric alternative. GBZ- and S1-mediated differences were statistically analyzed with one-way ANOVAs followed by post hoc Dunnett's correction or with a Kruskal–Wallis test followed by post hoc Dunn's correction. * $p < 0.05$, ** $p < 0.01$, *** $p < 0.001$, **** $p < 0.0001$.

mice. Only GBZ improved expression of ATF4-regulated markers in VWM mouse brain, whereas S1 did not, suggesting that it is the attenuation of ATF4-regulated mRNAs that contributes to improvement of VWM. This conclusion is in line with previous studies, which showed that reduction of effectors downstream of ATF4 is associated with amelioration of VWM.^{13,14}

A candidate target for GBZ's ISR- and disease-modulating capacity that is not shared with S1 could be the $\alpha 2$ -AR. One option is that stimulation of the $\alpha 2$ -AR changes intracellular cAMP concentrations.^{33,52,53} GADD34 expression can be regulated by cAMP levels,^{54,55} so GBZ could impact on GADD34 expression via modulating cAMP levels, leading to decreased eIF2 α

phosphorylation and lower expression of the ATF4 transcriptome. We investigated the expression of ATF4-regulated mRNAs, including *Gadd34*, in two AtT-20 lines that differ in expression of the $\alpha 2$ -AR. These experiments did not confirm GBZ- or $\alpha 2$ -AR-specific effects on these mRNAs. The potent $\alpha 2$ -AR agonist dexmedetomidine did not modulate their expression either (data not shown). This left us with the conclusion that GBZ has a particular effect on the ATF4 transcriptome in VWM mice that is not shared with S1. The deregulated ISR observed in VWM brain has not been successfully replicated in cell cultures, which hampers further mechanistic studies. Another option is that the $\alpha 2$ -AR-induced hypothermia contributes to GBZ therapeutic effect. Hypothermia elicits a cold-shock response that involves the coordinated cellular adaptation of transcription, translation, metabolism, cell cycle, and the cytoskeleton^{56,57} and includes suppression of the ATF4-regulated CHOP protein.⁵⁸ Possibly, GBZ-induced hypothermia attenuates the enhanced expression of the ATF4 transcriptome in VWM mouse brain. Temperature recordings have not been consistently described in preclinical GBZ studies, hampering firm interpretation of our findings in relation to previous studies. GBZ injections in VWM mice lacking the $\alpha 2$ -AR target could provide further insight.

GBZ, as an FDA approved and long-known safe drug, presents as a promising treatment option for patients with VWM. The striking beneficial effects of GBZ in VWM mice have led to the first clinical trial in VWM (<https://www.trialregister.nl/trial/7260> and <https://www.clinicaltrialsregister.eu/ctr-search/trial/2017-001438-25/NL>). Translating GBZ treatment into clinical studies comes with concerns regarding $\alpha 2$ -adrenergic side effects,⁵⁹ although rapid habituation is also seen in clinic⁶⁰ and dose levels with similar exposure as used in the current study have proven safe in adults. Our study makes clear that S1 is not simply a GBZ replacement without $\alpha 2$ -adrenergic effects for the treatment of VWM. Two other ISR-targeting molecules have shown marked ameliorating effects in VWM mice.^{13,14} These are novel compounds, delaying fast clinical development in young VWM patients. 2BAct caused morbidity in dogs and is not suitable for application in patients.¹⁴ ISRIB's efficacy is influenced by the specific eIF2B mutation¹³ and it may not be equally effective in all patients.⁶¹ The search for ISR-modulating compounds that do not bind eIF2B directly or cause dose-limiting side-effects remains important, because their efficacy is not expected to be affected by specific mutations in eIF2B and their use would benefit all VWM patients. Deciphering the GBZ ISR target and mechanism of action help in developing drugs lacking the $\alpha 2$ -adrenergic side effects. Studies that address the question which ISR components downstream of eIF2B

contribute to VWM pathophysiology and GBZ-mediated disease amelioration may help to identify other targets that can be exploited for future translational studies.

Acknowledgments

This study was supported by ELA grant 2017-02712 and ZonMW TOP grant 91211005. We thank Marcos Ross Adelman and Janneke Witvliet for their help with CatWalk; Vivi Heine, Stephanie Dooves, Timo ter Braak and Lisanne Wisse for helping with the first GBZ injections and downstream analyses of ISR mRNAs. We thank Professor Giuseppe Lauria Pinter (University of Milan, Italy) for providing guanabenz acetate and Professor Rob Henning (Rijksuniversiteit Groningen, the Netherlands) for sharing the temperature loggers. We thank Dr. Prashant Chittiboina (National Institute of Neurologic Diseases and Stroke, Bethesda, MD, USA) for sharing the AtT-20 cell line and Professor Lee Limbird (FISK University, Nashville, TN, USA) for sharing the AtT-20 cell line expressing $\alpha 2$ -AR. We thank the animal caretakers of the VU-VUmc animal facility for mouse breeding and advice. Marjo S. van der Knaap is a member of the European reference network for rare neurological disorders (ERN-RND), project ID 739510.

Conflict of Interest

MSvdK and TEMA have a patent PCT/NL2018/050293 on guanabenz in VWM pending to VUmc. Otherwise, the authors have declared no competing interest exists.

References

1. Hamilton EMC, van der Lei HDW, Vermeulen G, et al. The natural history of vanishing white matter. *Ann Neurol*. 2018;84:274-288.
2. Bugiani M, Boor I, van Kollenburg B, et al. Defective glial maturation in vanishing white matter disease. *J Neuropathol Exp Neurol*. 2011;70:69-82.
3. Dooves S, Bugiani M, Wisse LE, Abbink TEM, van der Knaap MS, Heine VM. Bergmann glia translocation: a new disease marker for vanishing white matter identifies therapeutic effects of Guanabenz treatment. *Neuropathol Appl Neurobiol*. 2018;44:391-403.
4. Dooves S, Bugiani M, Postma NL, et al. Astrocytes are central in the pathomechanisms of vanishing white matter. *J Clin Invest*. 2016;126:1512-1524.
5. van der Knaap MS, Leegwater PA, Konst AA, et al. Mutations in each of the five subunits of translation initiation factor eIF2B can cause leukoencephalopathy with vanishing white matter. *Ann Neurol*. 2002;51:264-270.
6. Wortham NC, Martinez M, Gordiyenko Y, Robinson CV, Proud CG. Analysis of the subunit organization of the

- eIF2B complex reveals new insights into its structure and regulation. *FASEB J.* 2014;28:2225-2237.
7. Konieczny A, Safer B. Purification of the eukaryotic initiation factor 2-eukaryotic initiation factor 2B complex and characterization of its guanine nucleotide exchange activity during protein synthesis initiation. *J Biol Chem.* 1983;258:3402-3408.
 8. Proud CG. Regulation of eukaryotic initiation factor eIF2B. *Prog Mol Subcell Biol.* 2001;26:95-114.
 9. Pakos-Zebrucka K, Koryga I, Mnich K, Ljujic M, Samali A, Gorman AM. The integrated stress response. *EMBO Rep.* 2016;17:1374-1395.
 10. Liu R, van der Lei HD, Wang X, et al. Severity of vanishing white matter disease does not correlate with deficits in eIF2B activity or the integrity of eIF2B complexes. *Hum Mutat.* 2011;32:1036-1045.
 11. van Kollenburg B, Thomas AA, Vermeulen G, et al. Regulation of protein synthesis in lymphoblasts from vanishing white matter patients. *Neurobiol Dis.* 2006;21:496-504.
 12. Horzinski L, Kantor L, Huyghe A, et al. Evaluation of the endoplasmic reticulum-stress response in eIF2B-mutated lymphocytes and lymphoblasts from CACH/VWM patients. *BMC Neurol.* 2010;10:94.
 13. Abbink TEM, Wisse LE, Jaku E, et al. Vanishing white matter: deregulated integrated stress response as therapy target. *Ann Clin Transl Neurol.* 2019;6:1407-1422.
 14. Wong YL, LeBon L, Basso AM, et al. eIF2B activator prevents neurological defects caused by a chronic integrated stress response. *Elife.* 2019;8. doi:10.7554/eLife.42940
 15. Wisse LE, Penning R, Zaal EA, et al. Proteomic and metabolomic analyses of vanishing white matter mouse astrocytes reveal deregulation of ER functions. *Front Cell Neurosci.* 2017;11:411.
 16. Terumitsu-Tsujita M, Kitaura H, Miura I, et al. Glial pathology in a novel spontaneous mutant mouse of the *Eif2b5* gene: a vanishing white matter disease model. *J Neurochem.* 2019;154:25-40. doi:10.1111/jnc.14887
 17. Han J, Back SH, Hur J, et al. ER-stress-induced transcriptional regulation increases protein synthesis leading to cell death. *Nat Cell Biol.* 2013;15:481-490.
 18. Holmes B, Brogden RN, Heel RC, et al. A review of its pharmacodynamic properties and therapeutic efficacy in hypertension. *Drugs.* 1983;26:212-229.
 19. Tsaytler P, Harding HP, Ron D, Bertolotti A. Selective inhibition of a regulatory subunit of protein phosphatase 1 restores proteostasis. *Science.* 2011;332:91-94.
 20. Das I, Krzyzosiak A, Schneider K, et al. Preventing proteostasis diseases by selective inhibition of a phosphatase regulatory subunit. *Science.* 2015;348:239-242.
 21. Wang L, Popko B, Tixier E, Roos RP. Guanabenz, which enhances the unfolded protein response, ameliorates mutant SOD1-induced amyotrophic lateral sclerosis. *Neurobiol Dis.* 2014;71:317-324.
 22. Chen Y, Podojil JR, Kunjamma RB, et al. Sephin1, which prolongs the integrated stress response, is a promising therapeutic for multiple sclerosis. *Brain.* 2019;142:344-361.
 23. Ng SY, Soh BS, Rodriguez-Muela N, et al. Genome-wide RNA-seq of human motor neurons implicates selective ER stress activation in spinal muscular atrophy. *Cell Stem Cell.* 2015;17:569-584.
 24. Tribouillard-Tanvier D, Béringue V, Desban N, et al. Antihypertensive drug guanabenz is active in vivo against both yeast and mammalian prions. *PLoS One.* 2008;3:e1981.
 25. Thapa S, Abdelaziz DH, Abdulrahman BA, Schatzl HM. Sephin1 reduces prion infection in prion-infected cells and animal model. *Mol Neurobiol.* 2020;57:2206-2219.
 26. Moreno JA, Radford H, Peretti D, et al. Sustained translational repression by eIF2 α -P mediates prion neurodegeneration. *Nature.* 2012;485:507-511.
 27. Crespillo-Casado A, Chambers JE, Fischer PM, Marciniak SJ, Ron D. PPP1R15A-mediated dephosphorylation of eIF2 α is unaffected by Sephin1 or Guanabenz. *Elife.* 2017;6:e26109.
 28. Hatzipetros T, Kidd JD, Moreno AJ, Thompson K, Gill A, Vieira FG. A quick phenotypic neurological scoring system for evaluating disease progression in the SOD1-G93A mouse model of ALS. *JoVE.* 2015;104:53257.
 29. Abbink TEM, Wisse LE, Jaku E, et al. Integrated stress response deregulation underlies vanishing white matter and is a target for therapy. *bioRxiv.* 2018;460840.
 30. de Veij Mestdagh CF, Timmerman JA, Koopmans F, et al. Torpor enhances synaptic strength and restores memory performance in a mouse model of Alzheimer's disease. *Sci Rep.* 2021;11:15486.
 31. Ladner CL, Yang J, Turner RJ, Edwards RA. Visible fluorescent detection of proteins in polyacrylamide gels without staining. *Anal Biochem.* 2004;326:13-20.
 32. Sabol SL. Storage and secretion of beta-endorphin and related peptides by mouse pituitary tumor cells: regulation by glucocorticoids. *Arch Biochem Biophys.* 1980;203:37-48.
 33. Surprenant A, Horstman DA, Akbarali H, Limbird LE. A point mutation of the α_2 -adrenoceptor that blocks coupling to potassium but not calcium currents. *Science.* 1992;257:977-980.
 34. Ruijter JM, Thygesen HH, Schoneveld OJ, et al. Factor correction as a tool to eliminate between-session variation in replicate experiments: application to molecular biology and retrovirology. *Retrovirology.* 2006;3:2.
 35. Caballero-Garrido E, Pena-Philippides J, Galochkina Z, et al. Characterization of long-term gait deficits in mouse dMCAO, using the CatWalk system. *Behav Brain Res.* 2017;331:282-296.

36. Young SK, Wek RC. Upstream open Reading frames differentially regulate gene-specific translation in the integrated stress response. *J Biol Chem.* 2016;291:16927-16935.
37. Lee YY, Cevallos RC, Jan E. An upstream open reading frame regulates translation of GADD34 during cellular stresses that induce eIF2 α phosphorylation. *J Biol Chem.* 2009;284:6661-6673.
38. Vieira FG, Ping Q, Moreno AJ, et al. Guanabenz treatment accelerates disease in a mutant SOD1 mouse model of ALS. *PLoS One.* 2015;10:e0135570.
39. Giovannitti JA Jr, Thoms SM, Crawford JJ. Alpha-2 adrenergic receptor agonists: a review of current clinical applications. *Anesth Prog.* 2015;62:31-39.
40. Breckenridge DG, Germain M, Mathai JP, Nguyen M, Shore GC. Regulation of apoptosis by endoplasmic reticulum pathways. *Oncogene.* 2003;22:8608-8618.
41. Yamaguchi S, Ishihara H, Yamada T, et al. ATF4-mediated induction of 4E-BP1 contributes to pancreatic beta cell survival under endoplasmic reticulum stress. *Cell Metab.* 2008;7:269-276.
42. Claes Z, Jonkhout M, Crespillo-Casado A, Bollen M. The antibiotic robenidine exhibits guanabenz-like cytoprotective properties by a mechanism independent of protein phosphatase PP1:PPP1R15A. *J Biol Chem.* 2019;294:13478-13486.
43. Buerkle H, Yaksh T. Pharmacological evidence for different α 2-adrenergic receptor sites mediating analgesia and sedation in the rat. *Br J Anaesth.* 1998;81:208-215.
44. Huang C, Ng OT, Chu JM, et al. Differential effects of propofol and dexmedetomidine on neuroinflammation induced by systemic endotoxin lipopolysaccharides in adult mice. *Neurosci Lett.* 2019;707:134309.
45. Tao L, Guo X, Xu M, et al. Dexmedetomidine ameliorates high-fat diet-induced nonalcoholic fatty liver disease by targeting SCD1 in obesity mice. *Pharmacol Res Perspect.* 2021;9:e00700.
46. Sundaram JR, Wu Y, Lee IC, et al. PromISR-6, a guanabenz analogue, improves cellular survival in an experimental model of Huntington's disease. *ACS Chem Neurosci.* 2019;10:3575-3589.
47. Ma Y, Hendershot LM. Delineation of a negative feedback regulatory loop that controls protein translation during endoplasmic reticulum stress. *J Biol Chem.* 2003;278:34864-34873.
48. Brush MH, Weiser DC, Shenolikar S. Growth arrest and DNA damage-inducible protein GADD34 targets protein phosphatase 1 α to the endoplasmic reticulum and promotes dephosphorylation of the α subunit of eukaryotic translation initiation factor 2. *Mol Cell Biol.* 2003;23:1292-1303.
49. Novoa I, Zeng H, Harding HP, Ron D. Feedback inhibition of the unfolded protein response by GADD34-mediated dephosphorylation of eIF2 α . *J Cell Biol.* 2001;153:1011-1022.
50. Novoa I, Zhang Y, Zeng H, Jungreis R, Harding HP, Ron D. Stress-induced gene expression requires programmed recovery from translational repression. *EMBO J.* 2003;22:1180-1187.
51. Jousse C, Oyadomari S, Novoa I, et al. Inhibition of a constitutive translation initiation factor 2 α phosphatase, CReP, promotes survival of stressed cells. *J Cell Biol.* 2003;163:767-775.
52. Hao Y, Tatonetti NP. Predicting G protein-coupled receptor downstream signaling by tissue expression. *Bioinformatics.* 2016;32:3435-3443.
53. Chabre O, Conklin BR, Brandon S, Bourne HR, Limbird LE. Coupling of the α 2A-adrenergic receptor to multiple G-proteins. A simple approach for estimating receptor-G-protein coupling efficiency in a transient expression system. *J Biol Chem.* 1994;269:5730-5734.
54. Arasi FP, Shahrestanaki MK, Aghaei M. A2a adenosine receptor agonist improves ER stress in MIN6 cell line through PKA/PKB/cAMP response element-binding protein and GADD34/eIF2 α pathways. *J Cell Physiol.* 2019;234:10500-10511.
55. Nakagawa T, Ohta K. Quercetin regulates the integrated stress response to improve memory. *Int J Mol Sci.* 2019;20:2761.
56. Adjirackor NA, Harvey KE, Harvey SC. Eukaryotic response to hypothermia in relation to integrated stress responses. *Cell Stress Chaperones.* 2020;25:833-846.
57. Al-Fageeh MB, Smales CM. Control and regulation of the cellular responses to cold shock: the responses in yeast and mammalian systems. *Biochem J.* 2006;397:247-259.
58. Zhu X, Zelmer A, Kapfhammer JP, Wellmann S. Cold-inducible RBM3 inhibits PERK phosphorylation through cooperation with NF90 to protect cells from endoplasmic reticulum stress. *FASEB J.* 2016;30:624-634.
59. Dalla Bella E, Bersano E, Antonini G, et al. The unfolded protein response in amyotrophic lateral sclerosis: results of a phase 2 trial. *Brain.* 2021;144:2635-2647.
60. Sica DA. Centrally acting antihypertensive agents: an update. *J Clin Hypertens.* 2007;9:399-405.
61. Slynko I, Nguyen S, Hamilton EMC, et al. Vanishing white matter: eukaryotic initiation factor 2B model and the impact of missense mutations. *Mol Genet Genomic Med.* 2021;9:e1593.
62. Wisse LE, Ter Braak TJ, van de Beek MC, et al. Adult mouse eIF2B ϵ Arg191His astrocytes display a normal integrated stress response in vitro. *Sci Rep.* 2018;8:3773.

Supporting Information

Additional supporting information may be found online in the Supporting Information section at the end of the article.

Figure S1 GBZ induces hypothermia which attenuates with a daily treatment regimen. Temperature loggers were inserted in 2-month-old, male WT and pre-symptomatic $2b4^{he}2b5^{ho}$ mice. Treatments of daily injection with 2.25% PEG300 (placebo), 4.5 mg/kg S1 (S1 D4.5), 4.5 mg/kg GBZ (GBZ D4.5) or weekly injection with 10 mg/kg GBZ (GBZ W10) were started 1 week after surgery for at least 14 days. Body temperature was registered once per hour (h). Mean baseline temperature for WT and $2b4^{he}2b5^{ho}$ mice were determined from placebo-injected animals (WT, 36.6°C, $2b4^{he}2b5^{ho}$, 35.4°C) and used for AUC calculations for each injection per animal. AUC indicates hypothermia and is based on temperature reduction and duration. Only after the first injection body temperatures did not recover to baseline before the next injection 24 h later. For this reason the AUC after the second injection was not included in statistical analyses. Graphs show mean AUC \pm SEM. * $p < 0.05$; **, ##, $p < 0.01$.

Figure S2 Myelin appearance in WT corpus callosum. WT mice were injected daily with placebo, 4.5 mg/kg S1 (S1 D4.5), 4.5 mg/kg GBZ (GBZ D4.5) or weekly with 10 mg/kg GBZ (GBZ W10). Sagittally cut brain sections of 2 WT mice were stained for MOG (brown) and counter stained with H&E (purple, indicating nuclei). Images show representative stainings of indicated sections per indicated treatment. Images of placebo-treated WT animals are taken from Figure 7 to serve as internal reference. Images are from the same section and represent one mouse per condition. White bars, 50 μ m.

Figure S3 Daily GBZ 4.5 mg/kg regionally ameliorates ATF4-regulated 4E-BP1 expression in the corpus callosum in $2b4^{he}2b5^{ho}$ mice. Images show representative immunohistochemistry for ATF4-regulated protein 4E-BP1 of indicated regions in the corpus callosum in $2b4^{he}2b5^{ho}$ (VWM) mice treated daily with placebo or 4.5 mg/kg GBZ (GBZ D4.5). Images are from the same sagittally cut section and represent one mouse per condition. Two mice were assessed. WT brain does not express 4E-BP1. Brown, 4E-BP1; purple, nuclei. White bars, 50 μ m.

Figure S4 GBZ and S1 attenuates *Xbp1* splicing in the absence or presence of the $\alpha 2$ -AR. (A) Verification of *Adra2a* mRNA levels in AtT-20 cell lines that express (+ $\alpha 2$) or do not express ($-\alpha 2$) $\alpha 2$ -AR subtype 2A, analyzed with an unpaired *t*-test. (B) Both cell lines were treated with vehicle (–) or thapsigargin (TG: +) for 6 h to induce ER stress, in the presence or absence of 50 μ mol/L S1 or 50 μ mol/L GBZ. ER stress activates *Ire1 α* and *ATF6*, which causes *Xbp1* mRNA splicing and upregulates expression of *Pdia4* mRNA, respectively.⁶² mRNA expression was quantified with qPCR (*Akt* as reference). *Xbp1* splicing was quantified as the ratio of spliced (s) and unspliced (u) to unspliced (u) *Xbp1*.⁶² Unexpectedly, *Pdia4* levels remained unaffected by TG in both AtT-20 cell lines, suggesting that *ATF6* was not induced by TG (data are therefore not included). Graphs indicate individual data points and means \pm SD. Differences between vehicle-treated versus TG-treated cells were analyzed with an unpaired *t*-test or the appropriate non-parametric alternative. GBZ- and S1-mediated differences were statistically analyzed with one-way ANOVAs followed by post hoc Dunnett's correction, a Welch's ANOVA or with a Kruskal–Wallis test. * $p < 0.05$, ** $p < 0.01$, **** $p < 0.0001$.

Table S1 Overview of number of animals per experiment with indicated tissue processing protocols.

Table S2 Primary antibodies.

Data S1 Result statistical analyses.

Data S2 CatWalk video of $2b4^{he}2b5^{ho}$ mouse treated with placebo.

Data S3 CatWalk video of $2b4^{he}2b5^{ho}$ mouse treated with GBZ4.5.

Data S4 CatWalk video of $2b4^{he}2b5^{ho}$ mouse treated with GBZ10.

Data S5 CatWalk video of WT mouse treated with placebo.

Data S6 CatWalk video of WT mouse treated with GBZ4.5.

Data S7 CatWalk video of WT mouse treated with GBZ10.